JOURNAL OF MATERIALS SCIENCE **34** (1999) 5449–5456

The effect of the thermal exposure on microstructure of MP159 alloy

SHIQIANG LU, BAOZHONG SHANG
Department of Materials Engineering, Nanchang Institute of Aeronautical Technology, Nanchang, 330034, People's Republic of China

ZIJIAN LUO
College of Materials Science and Engineering, Northwestern Polytechnical University, Xian, 710072, People's Republic of China

RENHUI WANG
Department of Physics Wuhan University, Wuhan, 430072, People's Republic of China

FANGCHANG ZENG
Aviation Industry Corporation, Beijing, 100034, People's Republic of China

The effect of the thermal exposure at different temperatures on the microstructure is investigated for MP159 alloy by optical microscopy and transmission electron microscopy (TEM). Thermal exposure at 660 °C is related to the aging induced hardening mechanism, thermal exposure at the neighborhood of 920 °C is associated with static recrystallization behavior, and thermal exposure at a temperature range of 920 to 1070 °C for a short time is investigated with a view toward obtaining the longest permissible thermal exposure time during which microstructural reconstitution of the cold deformed microstructure would not occur at the corresponding temperature, which would provide guidance for determining reasonable hot forging parameters of fasteners. The results indicate that both solution heat treated (ST) and cold worked (CW) MP159 alloy could be hardened by aging. This aging induced hardening is attributable to the precipitation of a very finely dispersed fcc ordered solid solution. The precipitating process is so rapid that the air cooling (AC) or water cooling (WC) process of the sample exposed to elevated temperature higher than normal aging temperature could produce an appreciable hardening effect. The recrystallization temperature of the alloy is as high as 920 °C, such a high recrystallization temperature is attributed to deformation twins and a variety of alloying elements due to their inhibition to the nucleation and growth of recrystallization grains, other than to the hcp-phase which used to be believed to explain high recrystallization temperature in MP alloys in some literature.

1. Introduction

MP159 alloy (containing 25.5Ni, 35.7Co, 19.0Cr, 9.0Fe, 7.0Mo, 3.0Ti, 0.6Nb, 0.2Al in wt %) is a latter number in the MULTIPHASE family of alloys (MULTIPHASE is a trademark of SPS Technologies, Inc., Newtown, PA). MP alloys are different from most of nickel-based and cobalt-based alloys, many of which derive their strength from the precipitation of gamma-prime or from solid-solution effects, whereas MP alloys derive their high strength from both cold working and aging. The first commercial alloy of MP alloys is MP35N (containing 35Co, 35Ni, 20Cr, 10Mo, in wt %) developed by Smith [1, 2]. Although MP35N possesses, like MP159, the unique combination of ultra-high strength, ductility and corrosion resistance, it has a relatively low service temperature (no higher than 300 °C) and a high mix cost, and it requires a considerable amount of cold work for hardening. In order to overcome these negative aspects, Slaney and Greenburg developed MP159 alloy [3, 4] which has a maximum service temperature of 593 °C.

There are many published papers investigating the strengthening mechanisms of cold working and aging for MP35N, but the conclusions are divergent [5–9], while the available literature on the strengthening mechanisms in MP159 is very limited. The cold working strengthening mechanisms in MP159 is not involved in the present investigation, and has been discussed in a separate publication [10]. The aging strengthening in this alloy, as a part of the present investigation, is investigated.

MP159 is at present widely used for critical fasteners which demand a combination of high strength and high resistance to corrosion [11, 12]. Because the material is already strengthened by cold working prior to bolt fabrication, the heads of bolts must be formed by hot

forging. In order to meet the requirement of the bolt application performance, the headed blanks must be free from recrystallization in the areas other than the head. From a easy forming point of view, the somewhat high forging temperature and somewhat long heating time are expected to obtain enough ductility. However, in order to prevent the cold deformed microstructure in the shank adjacent to the head from recrystallization due to heat conduction, the forging temperature is expected to be as low as possible, and the heating time as short as possible. In order to reach a balance between them, it is essential to investigate the static recrystallization behavior at different temperatures.

The present investigation has two purposes, one is to study age strengthening mechanisms in MP159, another is to investigate the static recrystallization behavior and to obtain the longest permissible thermal exposure time at different temperatures during which recrystallization of cold deformed microstructure do not occur, which can provide a guidance for determining reasonable hot forging parameters.

2. Experimental

The materials used in the present investigation are commercial cold drawn MP159 rods with 48% reduction of cross-section area. The diameter of the as-drawn rod is 10 mm. A typical producing schedule for MP159 is as follows: vacuum induction melted + vacuum consumable electrode melted + solution heat treated + cold drawn. The samples for optical metallography are etched with Kalling's reagent (100 cm^3 of absolute ethye alcohol, 100 cm^3 of hydrochloric acid (sp gr 1.19) and 5 g of cupric chloride) heated to about 60 °C. The samples for TEM are prepared by mechanical polishing followed by twin-jet electropolishing using a solution of 10% perchloric acid-absolute ethyl alcohol. TEM is performed using PHILPS-CM12 at 120 kV and JEOL-JEM-2000FXII at 200 kV.

Various thermal exposure tests are conducted in a high temperature furnace with silicon carbide heating elements. The furnace is heated to the selected temperature and held for three hours to obtain a uniform temperature in the chamber of the furnace, then sample is put into the chamber for selected time followed by AC or WC. In the commercial hot forging process of the heads of bolts, induction heating is generally used. Because induction heating rate is very rapid, the locally heated part by induction coil is approximately equivalent to the high temperature chamber, while the shank adjacent to the head of bolt which is not directly heated by induction coil is approximately equivalent to the samples put into the high temperature chamber. In other words, the microstructural changes in the shank adjacent to bolt head due to heat conduction are approximately equivalent to those in the samples exposed in high temperature chamber.

3. Results

3.1. Aging induced hardening

The Rockwell hardness of MP159 in ST and CW conditions are about HRC8 and HRC44, respectively (the lower values than HRC20 only for reference). However, the corresponding Rockwell hardness can be increased to about HRC18 and HRC52 respectively after aging heat treatment (660 °C for 4.15 h). The optical micrographs in the ST and CW conditions are shown in Fig. 1. The transmission electron micrgraph of CW sample is shown in Fig. 2. It can be seen that the ST microstructure consists of equiaxed fcc grains with a number of annealing twins, whereas the CW microstructure contains an intersecting network of very fine platelets in each fcc grain. In addition, relatively high dislocation density and dislocation tangle between thin platelets can be seen in CW condition. These platelets have been identified by authors to be deformation twins instead of hcp phase [10]. After aging of the ST and CW samples, no changes have been detected in optical micrographs and transmission electron micrographs (bright field (BF)). However, a careful diffraction work reveals the reflections of the precipitate in both ST + aged and CW + aged samples. Fig. 3 shows the selected-area electron diffraction pattern (SADP) in [0 0 1] matrix orientation and

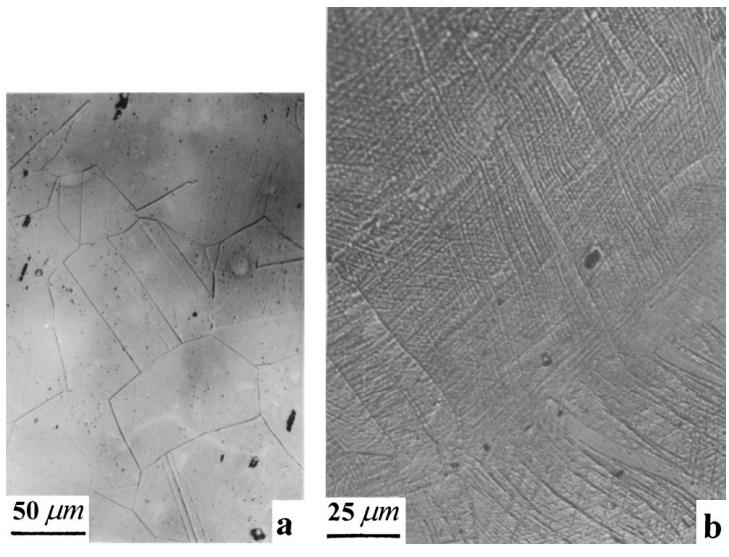

Figure 1 Optical micrographs: (a) ST, (b) CW.

corresponding dark-field (DF) image of the reflection of the precipitate for ST + aged sample, which indicats that the precipitate is very finely disperse distribution and is a fcc ordered solid solution. But BF image shows no signs of the precipitation. The SADPs in [0 0 1] and [1 1 1] matrix directions for the CW + aged sample are shown in Fig. 4. Fig. 4a demonstrates that the aged CW sample also produces the fcc ordered solid solution, but the intensity of the superlattice spots is relative weak.

Figure 2 Transmission electron micrograph in CW sample.

3.2. Static recrystallization behavior

The optical microstructures of the CW samples exposed to 910 °C for 30, 60 and 90 min have been examined. It is found that the deformed structure prior to thermal exposure remains unchanged. Fig. 5a shows the optical micrograph of the sample exposed to 910 °C for 1 h, no evidence of recrystallization can be seen. However, in the CW sample exposed to 920 °C for 2, 15, 30, 60 and 90 min, the development of the recrystallization can be clearly observed in the optical microscopy. Fig. 5b and c show light micrographs of the samples exposed to 920 °C for 2 and 30 min respectively. Fig. 5b indicates the recrystallization has already begun after only 2 min at 920 °C and the nucleation of recrystallization firstly occurs at the previous fcc grain boundaries. The volume fraction of recrystallized grains increases with time, but a complete recrystallization does not take place up to 1.5 h at 920 °C. Whereas for the sample exposed to 930 °C for only 30 min, a full recrystallization has taken place, as shown in Fig. 5d. It follows that the static recrystallization temperature of CW MP159 is 920 °C.

Fig. 6 shows the details of the recrystallization growth front for the sample exposed to 920 °C for 0.5 h

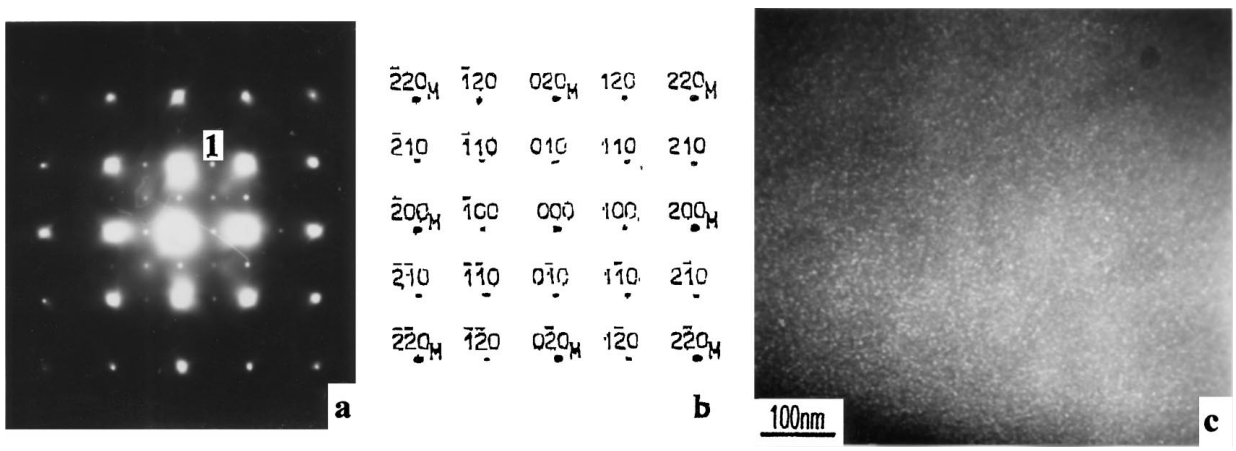

Figure 3 ST + aged sample: (a) SADP of [0 0 1] matrix orientation, (b) Key to (a), (c) DF from spot 1.

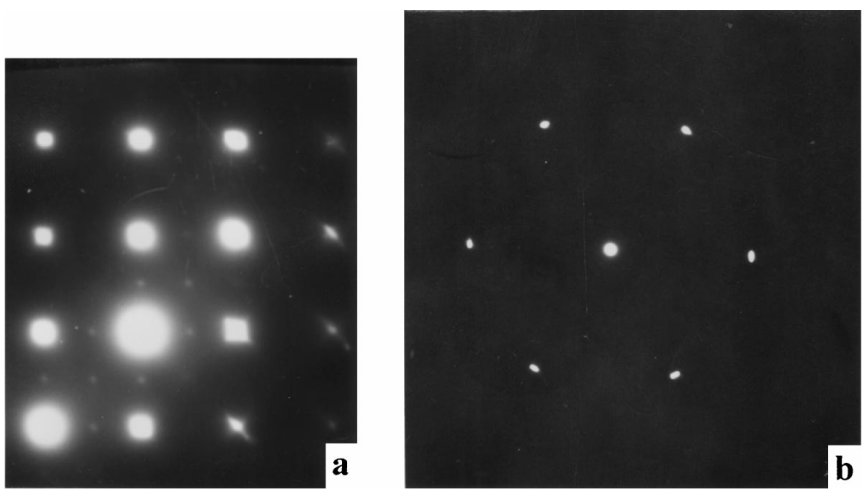

Figure 4 CW + aged sample: (a), (b) SADPs of [0 0 1] and [1 1 1] matrix orientations, respectively.

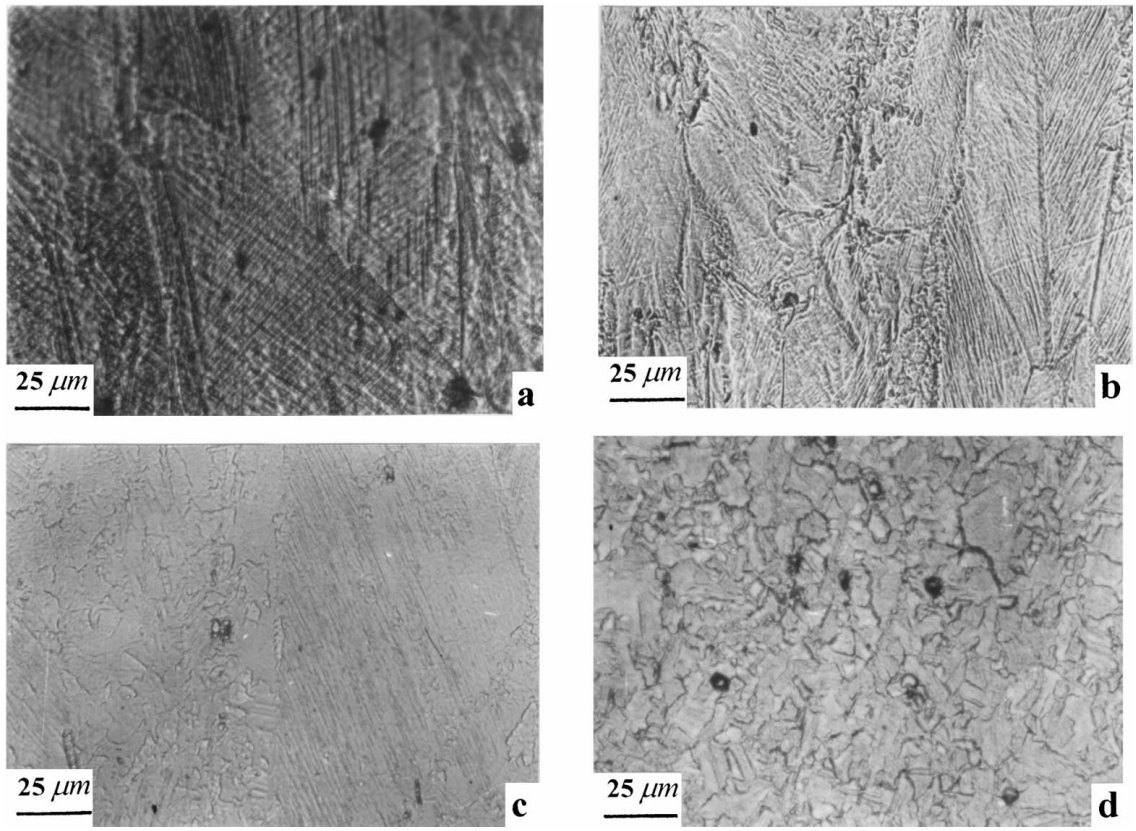

Figure 5 Microstructure of CW after exposure: (a) at 910 °C for 1 h, (b) at 920 °C for 2 min, (c) at 920 °C for 30 min, (d) at 930 °C for 30 min.

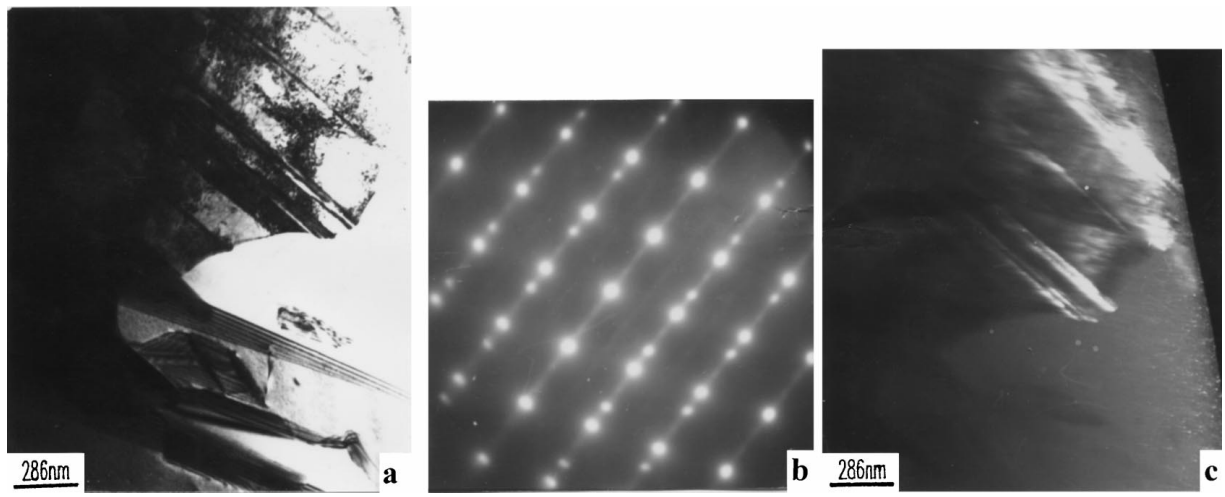

Figure 6 CW MP159 exposed to 920 °C for 30 min: (a) the interface between the recrystallization region and the deformed region, (b) corresponding SADP of [011] matrix orientation, (c) DF image from the reflection of twin.

and demonstrates that the platelets, which seem to be an inhibition to the growth of the recrystallization grains, are deformation twins other than hcp phase. Fig. 7 shows other details of the recrystallization growth front for the same sample and indicates that the deformation twin platelet parallel to the recrystallization front seems to have more effective inhibition to the growth of recryst allizing grains. Moreover, Fig. 7 still reveals clearly three deformation twin orientations, which correspond to twins on three of the four {1 1 1} type planes (the fourth being approximately parallel to the foil plane). In addition, weak long streak between two row matrix reflections along $[1\,\bar{1}\,1]_M$ direction can be seen in Figs 6b and 7e, which may be due to a very thin precipitate. This precipitate has been clearly observed in Fig. 8. According to Fig. 8b, it is know that the precipitate is an ordered hexagonal structure ($D0_{24}$), its *c* parameter is approximately twice that of hcp phase, so does its *a* parameter. It is not at present clear when the precipitate forms, a further investigation regarding it is required.

3.3. Elevated temperature short-time thermal exposure tests

After the head of bolt is formed by hot forging, the shank of the bolt must be free from recrystallization in order to retain the prior cold work strengthening effect. However, if the hot forging process is not reasonably

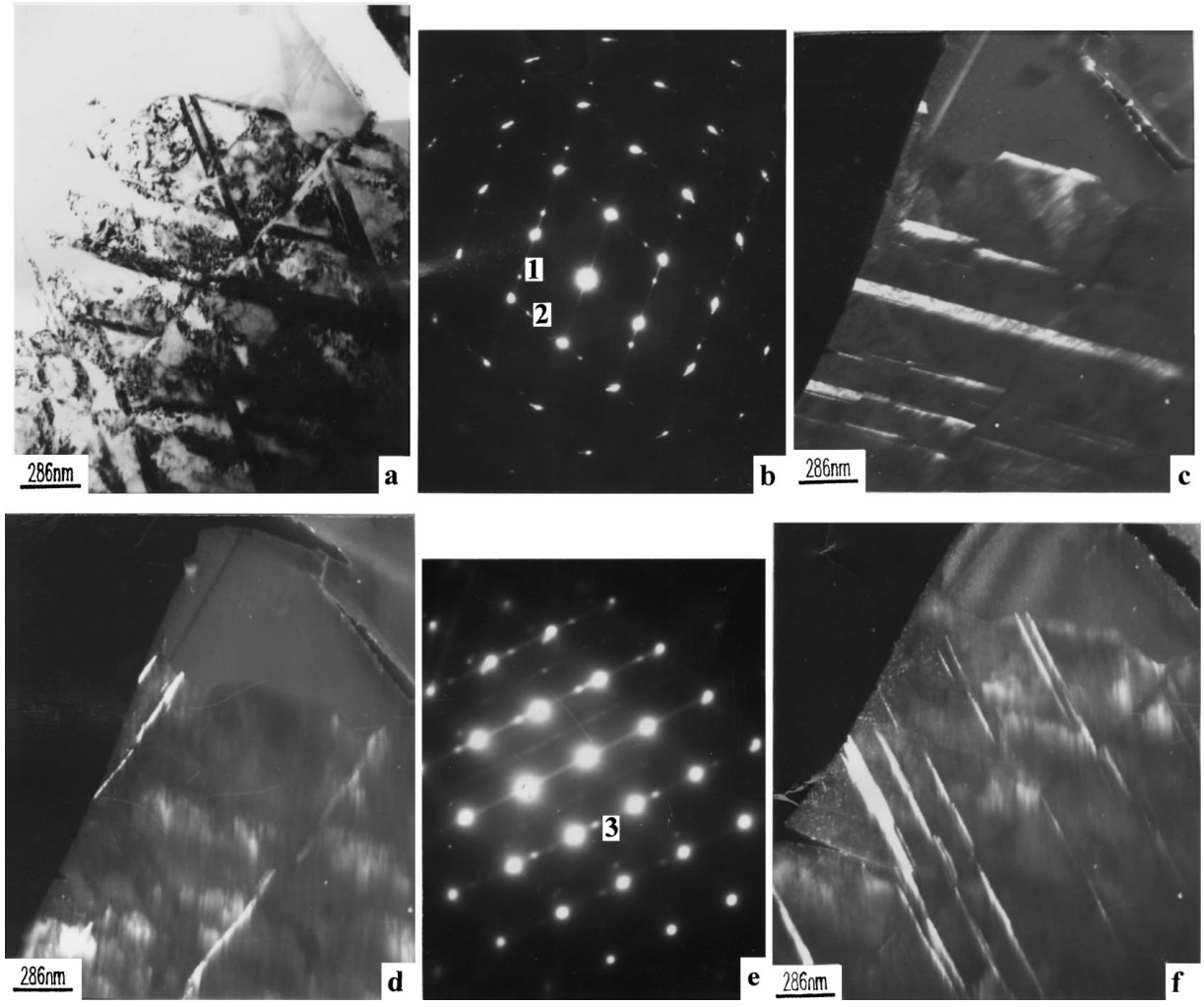

Figure 7 CW MP159 exposed to 920 °C for 30 min: (a) the interface between the recrystallization region and the deformed region, (b) corresponding SADP of [0 1 1] matrix orientation, (c) DF image of the twin reflection 1, (d) DF of twin reflection 2, (e) SADP of other ⟨0 1 1⟩ matrix orientation, (f) DF of twin reflection 3.

controlled, recrystallization may occur in the shank adjacent to the bolt head because of heat conduction. The present elevated temperature short-time thermal exposure tests are to simulate the thermal exposure situation of the shank near bolt head with a view toward obtaining the longest permissible thermal exposure time during which no recrystallization would occurs. These data can provide guidance for determining reasonable hot forging parameters.

According to the range of the forging temperatures determined by Shiqiang Lu *et al.* [13, 14], the thermal exposure temperatures are selected at the range of 920–1070 °C. The Rockwell hardness examination of all samples exposed to different temperatures for different time is shown in Table I. The microstructure of all exposed samples has been observed in the optical microscope. The examination of both the Rockwell hardness and the microstructure reveals that the changing of the microstructure coincides well with the changing of Rockwell hardness, the larger the volume fraction or the size of the recrystallized grains, the lower the Rockwell hardness. A relationship curve between the Rockwell hardness and the volume fraction of the recrystallized grains can be approximately drawn, as shown in Fig. 9. Generally, when Rockwell hardness is above the value of HRC44, no evidence of recrystallization can be seen, whereas when Rockwell hardness is below the value of HRC28, recrystallization has already finished and new grains begin to grow. On the basis of the examination of Rockwell hardness and optical microstructure, the longest permissible thermal exposure time for no occurrence of recrystallization at different temperatures is approximately as follows: 920 °C-100 s, 950 °C-90 s, 980 °C-70 s, 1010 °C- 60 s, 1040 °C-40 s, 1070 °C-20 s. It means that when the head of the bolt is formed at the above temperatures, the hot forging process must be finished within the corresponding permissible time, otherwise the recrystallization may occur in the shank near the head of the bolt.

In addition, it is strangely seen that although no microstructural changes can be seen by optical examination in the exposed samples in which no recrystallization occurs and in the CW sample prior to thermal exposure, the former has higher Rockwell hardness than the latter (the hardness of CW sample is about HRC44). Through careful electron diffraction work, the answer is found. As shown in Fig. 10, the superlattice spots of the fcc ordered solid solution in these thermally exposed samples is detected. It is this precipitate that resulted in the increase in Rockwell hardness. Obviously, the

TABLE I Rockwell hardness of thermally exposed samples

Temperature (°C) × Time (s)	920 × 90		920 × 120		920 × 180		920 × 360	
Cooling mode	AC	WC	AC	WC	AC	WC	AC	WC
Rockwell hardness (HRC)	49.8	48.3	44.2	43.4	38.2	37.1	29.8	28.8
Temperature (°C) × Time (s)	950 × 90		950 × 150		950 × 210		950 × 300	
Cooling mode	AC	WC	AC	WC	AC	WC	AC	WC
Rockwell hardness (HRC)	48.7	47.3	28.6	26.5	26.8	23.8	25.1	23.6
Temperature (°C) × Time (s)	980 × 90		980 × 120		980 × 150		980 × 180	
Cooling mode	AC	WC	AC	WC	AC	WC	AC	WC
Rockwell hardness (HRC)	43.2	42.3	28.1	26.2	26.6	25.4	25.1	24.3
Temperature (°C) × Time (s)	1010 × 40		1010 × 60		1010 × 90		1010 × 150	
Cooling mode	AC	WC	AC	WC	AC	WC	AC	WC
Rockwell hardness (HRC)	49.0	47.6	49.5	48.2	27.9	26.3	24.3	23.2
Temperature (°C) × Time (s)	1040 × 20		1040 × 40		1040 × 70		1040 × 120	
Cooling mode	AC	WC	AC	WC	AC	WC	AC	WC
Rockwell hardness (HRC)	48.6	47.6	50.1	48.8	30.5	27.2	23.4	18.3
Temperature (°C) × Time (s)	1070 × 20		1070 × 40		1070 × 90		1070 × 120	
Cooling mode	AC	WC	AC	WC	AC	WC	AC	WC
Rockwell hardness (HRC)	49.2	48.8	34.6	33.2	24.3	23.4	17.9	15.0

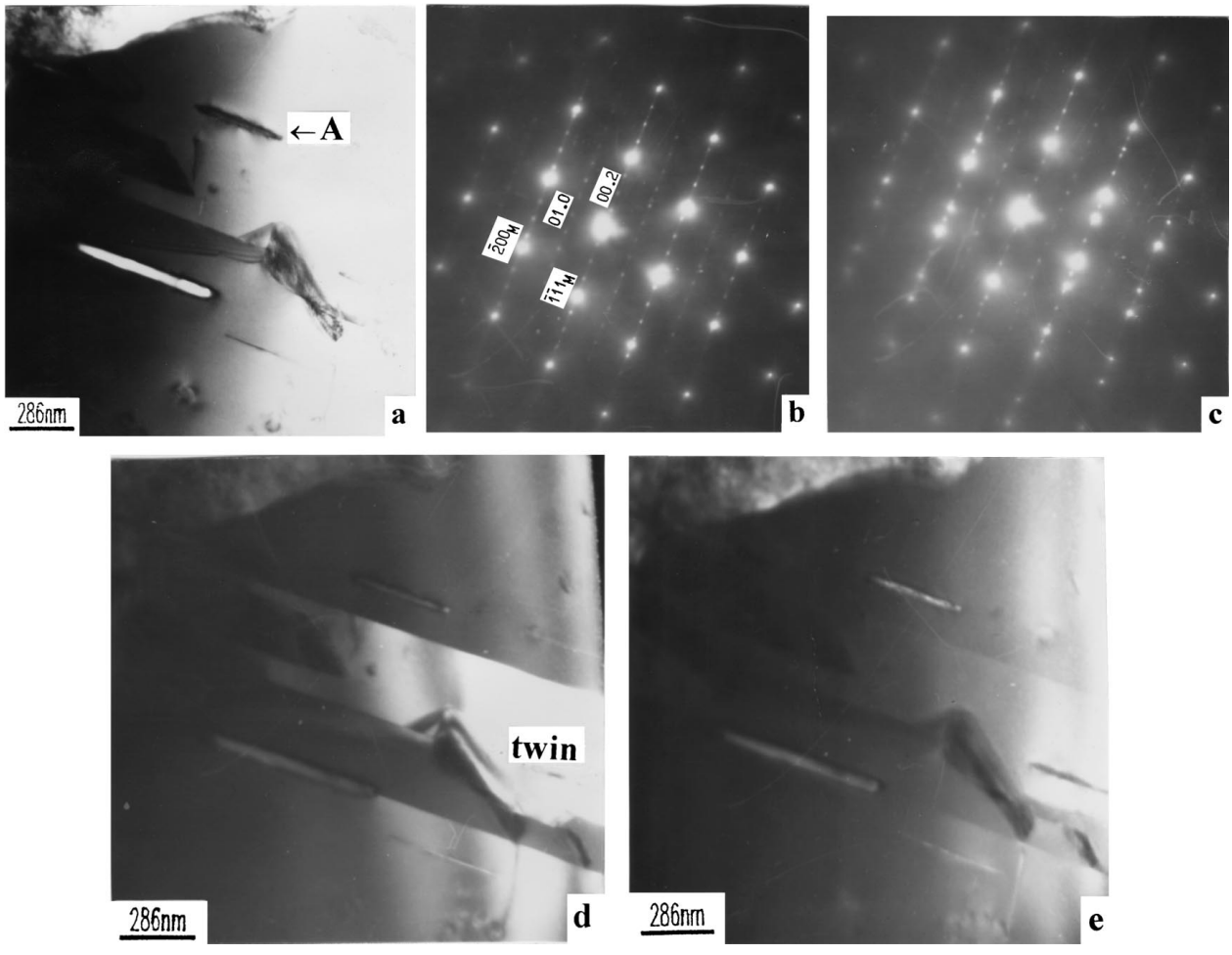

Figure 8 CW MP159 exposed to 920 °C for 30 min: (a) BF image (recrystallized region), (b) SADP of [0 1 1] matrix direction (containing platelet A), (c) SADP of [0 1 1] matrix direction (containing platelet A and annealing twin), (d) DF image of twin reflection, (e) DF image of the platelet A reflection.

precipitate forms during the cooling process, which indicates that the formation of the fcc ordered solid solution is very rapid. Such a rapid formation coincides with the observation in MP35N by Drapier *et al.* [6] that age hardening reaches its maximum value after only 15 min. Another superficially strange phenomenon is that, for the same thermal exposure, the sample cooled by air has somewhat higher hardness than the one cooled by water (see Table I), although their optical microstructure are identical. The electron diffraction work demonstrates it is also associate with the precipitation phase. Since the samples by AC have more time for the formation of the precipitate than those by WC in the aging temperature range, the former could produce more precipitate than the latter, that is why the hardness of the former is somewhat higher than the latter.

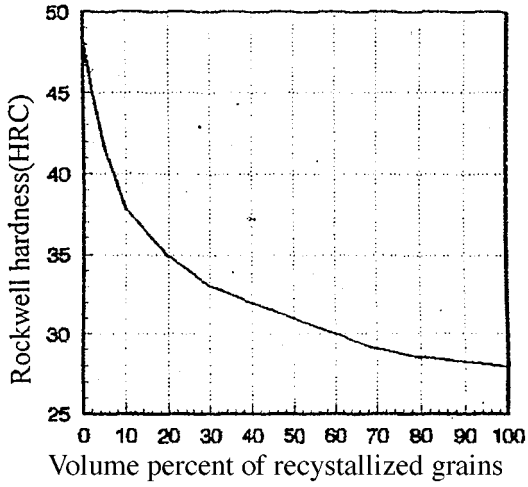

Figure 9 Relationship between Rockwell hardness and volume fraction of recrystallized grains.

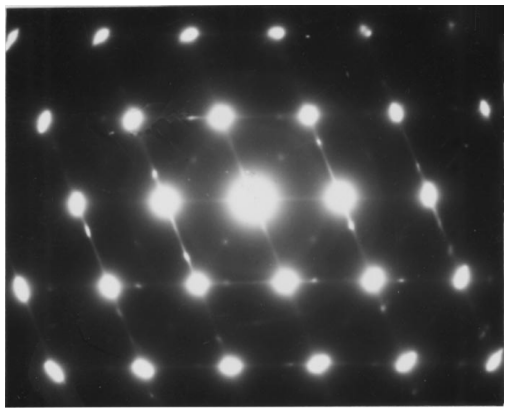

Figure 10 SADP of [0 1 1] matrix direction in CW sample exposed to 1040 °C for 40 s and followed by AC.

4. Discussion

The physical origin of the age hardening in MP alloys is not well understood. Many researchers have investigated age hardening mechanisms in MP35N, but the conclusions, as mentioned previously, are divergent. Graham [5] pointed out that the age hardening in CW MP35N was attributed to the precipitation of Co_3 Mo, an ordered hexagonal phase ($D0_{19}$) whose *c* parameter is approximately equal to that of hcp phase and whose *a* is approximately twice that of hcp phase, whereas the age hardening in ST MP35N was absent due to no formation of the precipitate. Graham thought that the hcp platelets formed during cold work acted as nucleation site and was necessary condition for the precipitation of Co_3 Mo. In agreement with the above conclusion, Drapier *et al.* [6] also demonstrated that the age hardening in MP35N resulted from the precipitation of Co_3 Mo. However, Raghavan *et al.* [7] and Singh *et al.* [8] obtained different conclusions in their investigation. The investigation by Raghavan *et al.* showed that no hcp platelets were found in CW MP35N, neither did Co_3 Mo in CW+aged MP35N, but the precipitation of ε-platelets, which were believed to be responsible for the age hardening, was detected in CW+aged MP35N. While the investigation by Singh *et al.* presented that no changes were seen in either hardness or microstructure in ST+aged MP35N, but age hardening in CW+aged MP35N was seen, however, no microstructural changes associated with this secondary hardening could be detected, although CW microstructure contained hcp-platelets which were regarded as nucleation site of Co_3 Mo by Graham and Drapier *et al.* [5, 6]. Therefore, Singh *et al.* [8] thought that age hardening of CW MP35N might arise from local solute partitioning between the matrix and hcp phase, but it is not so far clear how solute partitioning could give rise to the age hardening.

The investigation performed by the above investigators has showed that, the age treatment has no hardening effect for ST MP35N, while same treatment has obvious age hardening effect for CW MP35N, although the physical origin of this hardening is divergent in explanation. The present investigation for MP159 indicates that the age treatment can result in hardening for both ST and CW conditions. The careful diffraction work reveals the existence of a finely disperse fcc ordered solid solution (see Figs 3, 4 and 10), i.e. Ni_3 X, which has a molecular formula of $(Ni,Co,Fe,Cr,Mo)_3$ (Al,Ti,Nb) [15] but could not be seen in optical microscopy and TEM(BF). No evidence of the formation of Co_3 Mo has been seen in both ST+aged and CW+aged MP159, which is in agreement with Graham's opinion [5] because of the absence of suitable nucleation site for Co_3 Mo. The precipitation of ε-platelets, as reported by Raghavan [7], is not detected either in MP159 because, if this precipitate existed, the reflections of ε-platelets should have occurred in the SADP of [1 1 1] matrix orientation. As shown in Fig. 4b, only matrix reflections appeared in the SADP of [1 1 1] matrix orientation. In addition, the precipitate which has an ordered hexagonal structure ($D0_{24}$) and is discovered in Fig. 8 has not been detected either in CW+aged sample because its superlattice sports are absent in Fig. 4b.

Guangwei Han *et al.* [16] thought age hardening of CW MP159 came partially from the volume fraction increase of hcp platelets, which was established on the basis that large amounts of hcp platelets were formed during cold deformation. In fact, the intersecting network of fine platelets in CW MP159 is deformation twin platelets other than hcp-phase [10], which is also further supported by Figs 6, 7 and 10. Furthermore, in Guangwei Han *et al.* article [16], two sets of SADPs used to support their conclusion are, in fact, composite patterns of [4 1 1] matrix orientation, the corresponding extra spots from platelets are the reflections of the twin platelets, but they mistakenly regarded these SADPs as those of [0 1 1] matrix orientation and the extra sports were also mistakenly regarded as reflections of hcp platelets. Therefore, their conclusion that age hardening result, in part, from the volume fraction increase of hcp platelets is incorrect.

On the basis of the present experimental observation and the above discussion, it can be conclued that both ST and CW MP159 alloy could be hardened by aging because of the precipitation of very finely disperse fcc ordered solid solution.

Singh *et al.* [8] and Guangwei Han *et al.* [17] thought that the relative high recrystallization temperature in the MP alloys was due to the inhibition of hcp platelets to the growth of the recrystallizing grains, which comes from interfacial energy increasing because of the coherent interfaces of the hcp phase (0 0 0 1) // {1 1 1}

becoming incoherent interfaces, and thought that deformation twin platelets provide no resistance to recrystallization because of no energy barrier to consumption of the single twinned structure by the recrystallization front. But the present investigation results in MP159 are incompatible with the above conclusions. As mentioned previously, there are no hcp platelets in CW MP159. Furthermore, even if there were hcp platelets, these hcp platelets would dissolve when heated to the temperature higher than 704 °C because the fcc/hcp transus of MP159 is below 704 °C [18]. On the other hand, Singh *et al.* [8] and Guangwei Han *et al.* [17] did not identify by the diffraction work that the platelets, which seemed to inhibit growing of the recrystallization grains, were really hcp platelets. So their conclusions were unreliable.

It is well known that the fcc structure recrystallizes by passage of a high-angle grain boundary through the deformed fcc matrix. While for deformation twin platelets, the fcc structure may recrystallize by passage of the high-angle grain boundary through twin platelets or bypassing the twin platelets, which is related to the orientations of the twin platelets and the recrystallization front. When recrystallization front bypasses the twin platelets, the twin platelets also provide the inhibition to the growth of the recrystallizing grains (see Figs 6 and 7). This inhibition is attributable to the increasing of the interfacial energy due to the change of the coherent twin interfaces into incoherent twin interfaces. Although the deformation twins have the effect of inhibiting the growing of recrystallization grains, such high recrystallization temperature of 920 °C does not result from this inhibition alone. For example, CW MP35N, although there are a number of deformation twins [7] or both deformation twins and hcp phase [8], has a recrystallization temperature of about 808 °C. Because MP159 has a more complex chemical composition than MP35N, another cause may be a variety of alloying elements in MP159. These alloying elements inhibit cross slip of the dislocations, consequently, inhibiting the nucleation and growth of the recrystallization grains [19]. Therefore, it can be concluded that both deformations twins and a variety of alloying elements in MP159 result in such a high recrystallization temperature of 920 °C.

5. Conclusions

1. Both solution treated and cold worked MP159 can be hardened by aging heat treatment. The aging induced hardening is attributed to the precipitation of Ni_3 X, a fcc ordered solid solution, which cannot be detected in the optical micrograph and transmission electron micrograph (bright field). Only careful electron diffraction work can reveal its presence because of its very fine disperse distribution. The formation of the precipitate is very rapid. A certain amount of precipitate can form only during air or water cooling process of the sample exposed to elevated temperature for a short time, and produces an appreciable hardening effect.

2. MP159 alloy has a high recrystallization temperature of 920 °C. Such a high recrystallization temperature is attributable to both the inhibition of a variety of alloying elements to the nucleation and growth of recrystallization grains and the obstruction of deformation twins to the growth of the recrystallization grains, rather than to the hcp-phase which was generally believed to be responsible for the high recrystallization temperature of MP alloys in some literature.

3. In order to prevent the cold worked MP159 from recrystallization, the longest permissible thermal exposure time at different temperatures are approximately as follows: 920 °C-100 s, 950 °C-90 s, 980 °C-70 s, 1010 °C-60 s, 1040 °C-40 s, 1070 °C-20 s. It means that when the head of the bolt is formed at the above temperatures, the hot forging process must be finished within the corresponding permissible time, or the recrystallization may occur in the shank adjacent to the head of the bolt due to heat conduction.

4. The precipitate of the ordered hexagonal $D0_{24}$ is first found in the CW MP159 alloy exposed to 920 °C for 30 min. A further investigation regarding it is required.

Acknowledgements

The authors would like to thank X. W. Liu, X. L. Wu (China Geological University) and P. H. Li, M. B. Wen (Iron and Steel Institute of Wuhan Iron and Steel Corporation) for asistance in TEM. Thanks are also due to An Hu Mechanical Factory for supplying the commerical 48% cold drawn MP159 alloy.

References

1. G. D. SMITH, US Patent no. 3,356,542 (1967).
2. *Idem.*, US Patent no. 3,562,024 (1971).
3. J. S. SLANEY, US Patent no. 3,767,385 (1973).
4. J. S. SLANEY and R. A. NEBIOLO, *Metall.* **16** (1983) 137–161.
5. A. H. GRAHAM, *Trans. of the ASM* **62** (1969) 930–935
6. J. M. DRAPIER, P. VIATOUR, D. COUTSOURADIS and L. HABRAKEN, *Cobalt* **49** (1970) 171–186.
7. M. RAGHAVAN, B. J. BERKOWITZ and R. D. KANE, *Metall. Trans.* **11A** (1980) 203–207.
8. R. P. SINGH and R. D. DOHERTY, *ibid.* **23A** (1992) 307–319.
9. A. H. GRAHAM and J. L. YOUNGBLOOD, *ibid.* **1** (1970) 423–430.
10. SHIQIANG LU, BAOZHONG SHANG, ZIJIAN LUO, RENHUI WANG and FANGCHANG ZENG, to be published.
11. L. KLINE and M. LAWER, *Mater. Eng.*, **106** (1989) 55–56.
12. *Idem.*, Aircr. Eng. Aerosp. Technol. **61** (1989) 2–4.
13. SHIQIANG LU, BAOZHONG SHANG, ZIJIAN LUO, FANGCHANG ZENG and YU LIU, *Mater. Sci. Technol.* **6** (1998) 41–45 (in Chinese).
14. *Idem., J. of Plasticity Engineering* **5** (1998) 3–7 (in Chinese).
15. MA SHUPO, ZHANG YUN, CHANG XIN and ZHOU JING, *J. Mater. Eng.* **4** (1990) 35–37 (in Chinese).
16. GUANGWEI HAN, DI FENG, MING YIN and NANSENG YANG, *J. Mater. Sci. Technol.* **12** (1996) 109–113.
17. GUANGWEI HAN, DI FENG, MING YIN, WUJUN YE and HELI LUO, *ibid.* **12** (1996) 277–280.
18. F. C. HAGAN, H. W. ANTES, M. D. BOLDY and J. S. SLANEY, "Superalloyes" (TMS-AIME, Warrendale, PA, 1984) 621–630.
19. GENGXIANG HU and MIAOGEN QIAN, "Physical Metallurgy" (Shanghai Science and Technology Press, Shanghai, 1980) pp. 319–322 (in Chinese).

Received 29 December 1998
and accepted 21 April 1999